

Electronic Supplementary Information (ESI) for

## **Mesoporous palladium-boron alloy nanospheres**

Hao Lv,<sup>a</sup> Lizhi Sun,<sup>a</sup> Dongdong Xu,<sup>\*a</sup> Joel Henzie,<sup>b,c</sup> Yusuke Yamauchi,<sup>\*b,d,e</sup> and Ben Liu<sup>\*a</sup>

<sup>a</sup>Jiangsu Key Laboratory of New Power Batteries, Jiangsu Collaborative Innovation Center of Biomedical Functional Materials, School of Chemistry and Materials Science, Nanjing Normal University, Nanjing 210023, China

E-mail: ddxu@njnu.edu.cn; ben.liu@njnu.edu.cn

<sup>b</sup>Key Laboratory of Eco-chemical Engineering, College of Chemistry and Molecular Engineering, Qingdao University of Science and Technology, Qingdao 266042, China

<sup>c</sup>International Center for Materials Nanoarchitectonics (WPI-MANA), National Institute for Materials Science (NIMS), 1-1 Namiki, Tsukuba, Ibaraki 305-0044, Japan

<sup>d</sup>School of Chemical Engineering and Australian Institute for Bioengineering and Nanotechnology (AIBN), The University of Queensland, Brisbane, QLD 4072, Australia  
E-mail: y.yamauchi@uq.edu.au

<sup>e</sup>Department of Plant & Environmental New Resources, Kyung Hee University, 1732 Deogyong-daero, Giheung-gu, Yongin-si, Gyeonggi-do 446-701, South Korea

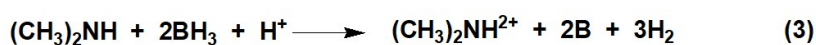
## 1. Chemicals and Materials

Palladium(II) chloride (PdCl<sub>2</sub>, 99.9 wt%), potassium tetrachloroplatinate (K<sub>2</sub>PtCl<sub>4</sub>), silver nitrate (AgNO<sub>3</sub>), copper nitrate (Cu(NO<sub>3</sub>)<sub>2</sub>), commercial palladium nanoparticles (Pd NPs), dioctadecyldimethylammonium chloride (DODAC), cetyltrimethylammonium chloride (C<sub>16</sub>TAC), octadecyl trimethyl ammonium chloride (C<sub>18</sub>TAC), Pluronic F127, orthoboric, ascorbic acid (AA), ammonium fluoride (NH<sub>4</sub>F), boric acid (H<sub>3</sub>BO<sub>3</sub>) and borane dimethylamine complex (DMAB) were obtained from Alfa Aesar. Nafion solution, commercial Pd and Pt nanoparticles on carbon were obtained from Sigma Aldrich. Hydrochloric acid (HCl), ammonium solution (NH<sub>3</sub>·H<sub>2</sub>O), and sodium hydroxide (NaOH) were purchased from Sinopharm Chemical Reagent Co. Ltd. (shanghai). C<sub>22</sub>TAC was synthesized according to our previous report.<sup>S1</sup> 10 mM H<sub>2</sub>PdCl<sub>4</sub> solution was prepared by dissolving 0.355 g of palladium (II) chloride into 20 mL of 0.2 M HCl solution and further diluting with 180 mL of deionized H<sub>2</sub>O. All the reagents are of analytical reagent grade and used without further purification. Deionized H<sub>2</sub>O with the resistivity of 18.25 mΩ was used in all experiments.

## 2. Synthesis of Pd-B and PdM-B (M = Cu, Ag, Pt) mesoporous nanospheres

Binary Pd-B mesoporous nanospheres (MNSs) were synthesized by a solution-phase route using DODAC as the surfactant template, H<sub>2</sub>PdCl<sub>4</sub> as the metal precursor, H<sub>3</sub>BO<sub>3</sub> and DMAB as the B sources and reducing agents at 75 °C. In a typical synthesis, 30 mg of DODAC was dissolved in 10 mL of deionized H<sub>2</sub>O to obtain a homogeneous solution at 25 °C, followed by the addition of 1 mL of NH<sub>4</sub>F solution (0.337 M), 1 mL of H<sub>3</sub>BO<sub>3</sub> solution (0.101M), 0.8 mL of H<sub>2</sub>PdCl<sub>4</sub> solution (10 mM) under gently shaking. After 5 min, 0.4 mL of NH<sub>3</sub>·H<sub>2</sub>O (2.5 wt.%) was injected to adjust the pH of the solution. The color of the solution changed from pink to colorless directly. Then, the solution was moved into an oven and further incubated at 75 °C for 30 min. Binary Pd-B MNSs were then obtained by the injection of 1.0 mL of freshly prepared DMAB (0.1 M) into above solution, followed by the color change from colorless to dark brown immediately. Lastly, the product was collected by centrifugation and washed several times with ethanol/H<sub>2</sub>O. Meanwhile, pH, reaction temperatures, and the species of surfactants were also tuned to control the nanostructures of as-resulted Pd-B MNSs under the similar procedures. Besides, ternary PdCu-B MNSs, PdAg-B MNSs and PdPt-B MNSs were synthesized using the above procedures, except one more metal precursor was added (Cu(NO<sub>3</sub>)<sub>2</sub>, AgNO<sub>3</sub>, K<sub>2</sub>PtCl<sub>4</sub>, respectively).

The formation mechanism of binary Pd-B nanoalloys:<sup>S2,S3</sup>



(CH<sub>3</sub>)<sub>2</sub> BH<sub>3</sub> reacts with OH<sup>-</sup> to form BH<sub>3</sub>OH<sup>-</sup> which acts as the real reducing agent during the crystallization. Then, PdCl<sub>4</sub><sup>2-</sup> and BH<sub>3</sub> co-reduced and formed binary Pd-B nanoalloys.

### 3. Electrochemical EOR measurements

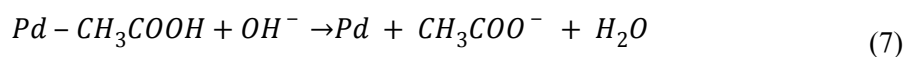
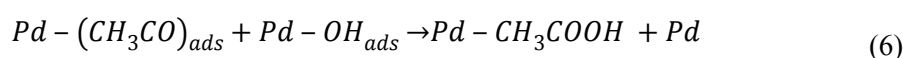
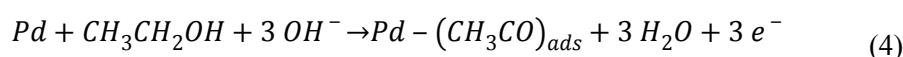
Electrocatalytic ethanol oxidation reaction (EOR) tests were performed on the CHI 660E electrochemical analyzer at 25 °C, followed by our previous works.<sup>S4,S5</sup> A three-electrodes system was used for all electrochemical tests, in which glassy carbon electrode (GCE, 0.07065 cm<sup>2</sup>) was used as the working electrode, a carbon rod as the counter electrode, and a Ag/AgCl electrode as the reference electrode. Before electrochemical characterizations, as-synthesized Pd-based mesoporous nanocatalysts were cleaned with acetic acid for three times and ethanol/H<sub>2</sub>O for three times also to remove the surfactants.<sup>S6</sup> Then, obtained nanocatalysts were freeze-dried at -60 °C. An ink of the catalysts was prepared by mixing 1 mg of nanocatalysts, 4 mg of Vulcan XC-72 carbon, 1.5 mL of ethanol and 0.5 mL of H<sub>2</sub>O. After sonicating for 0.5 h, 50 μL of Nafion solution (5 wt% in alcohol and H<sub>2</sub>O) was added and further sonicated for 0.5 h. Then, 6 μL of above-prepared ink solution (3 μg of the catalyst) was dropped on the GCE electrode and dried at 40 °C before test. Cyclic voltammograms (CVs) were then scanned until the stabilized curves were obtained for further removal of the surfactant in 1.0 M KOH.<sup>S7</sup> CVs were used to evaluate the electrochemical surface areas (1.0 M KOH) and activities (1.0 M KOH and 1.0 M ethanol) of the nanocatalysts at different scan rates and temperatures. The electrolyte solution was initially purged with N<sub>2</sub> for 30 min to remove O<sub>2</sub> and other gas before test. For CO stripping tests, the work electrode containing 3 μg of the catalyst was immersed in 1 M KOH solution. Then, CO was purged in the solution for 30 min to achieve the maximum coverage of CO at a fixed potential of 0.15 V (SCE). After that, the electrode was moved into fresh N<sub>2</sub>-purged 1.0 M KOH solution for CO stripping measurements. CO stripping voltammetry was recorded in the potential range between -0.9 and 0.2 V at a scan rate of 50 mV s<sup>-1</sup>.

ECSAs of the Pd-B MNSs were calculated from CVs in the area of PdO reduction peaks in 1.0 M KOH with a scan rate of 50 mV/s (Fig. S9a). The corresponding calculated equation is:

$$ECSA = \frac{Q_{PdO}}{0.405 \text{ mC cm}^{-2} \times m_{Pd}}$$

where  $Q_{PdO}$  is the charge by integrated the reduction peak area of PdO to Pd, 0.405 mC cm<sup>-2</sup> is the charge for the reduction of PdO, and  $m_{Pd}$  is the mass of Pd on the electrode.

Ethanol electrooxidation proceeds on the Pd catalysts according to the following mechanisms:<sup>S4,S7,S8</sup>



The rate-determining step of electrochemical EOR is the oxidation/removal of poisoning carbonaceous intermediates on Pd (Pd-(CH<sub>3</sub>CO)<sub>ads</sub>) by adsorbed OH (OH<sub>ads</sub>) (Eq. 6).

#### 4. Characterizations

Transmission electron microscopy (TEM) and high-resolution TEM studies were carried out using a JEOL 2010 TEM with an accelerating voltage of 200 kV. High-angle annular dark-field scanning TEM (HAADF-STEM) and corresponding line scan were performed on FEI Talos F200X apparatuses at an accelerating voltage of 200 kV, which are equipped with STEM and EDS detectors for elemental mapping analysis. TEM and STEM samples were prepared by casting a suspension of the samples (in ethanol and/or H<sub>2</sub>O) on a carbon coated copper grid (300 mesh). X-ray diffraction (XRD) patterns were collected on the powder samples using a D/max 2500 VL/PC diffractometer (Japan) equipped with graphite-monochromatized Cu K $\alpha$  radiation. X-ray photoelectron spectra (XPS) were performed on a scanning X-ray microprobe (Thermo ESCALAB 250Xi) that uses Al K $\alpha$  radiation. The binding energy of the C 1s peak (284.8 eV) was employed as a standard to calibrate the binding energies of other elements. Inductively coupled plasma mass spectrometry (ICP-MS) was recorded on a NexION 350D.

#### Supporting References

- (S1) Xu, D.; Liu, X.; Lv, H.; Liu, Y.; Zhao, S.; Han, M.; Bao, J.; He, J.; Liu, B. Ultrathin Palladium Nanosheets with Selectively Controlled Surface Facets. *Chem. Sci.* **2018**, *9*, 4451-4455.
- (S2) Wang, J.-Y.; Kang, Y.-Y.; Yang, H.; Cai, W.-B. Boron-doped palladium nanoparticles on carbon black as a superior catalyst for formic acid electro-oxidation. *J. Phys. Chem. C* **2009**, *113*, 8366-8372.
- (S3) Jiang, K.; Xu, K.; Zou, S.; Cai, W.-B. B-Doped Pd catalyst: boosting room-temperature hydrogen production from formic acid-formate solutions. *J. Am. Chem. Soc.* **2014**, *136*, 4861-4864.
- (S4) Lv, H.; Lopes, A.; Xu, D.; Liu, B. Multimetallic Hollow Mesoporous Nanospheres with Synergistically Structural and Compositional Effects for Highly Efficient Ethanol Electrooxidation. *ACS Cent. Sci.* **2018**, *4*, 1412-1419.
- (S5) Lv, H.; Sun, L.; Zou, L.; Xu, D.; Yao, H.; Liu, B. Size-Dependent Synthesis and Catalytic Activities of Trimetallic PdAgCu Mesoporous Nanospheres in Ethanol Electrooxidation. *Chem. Sci.* **2019**, *10*, 1986-1993.
- (S6) Fan, Q.; Liu, K.; Liu, Z.; Liu, H.; Zhang, L.; Zhong, P.; Gao, C. A Ligand-Exchange Route to Nobel Metal Nanocrystals with a Clean Surface for Enhanced Optical and Catalytic Properties. *Part. Part. Syst. Charact.* **2017**, *34*, 1700075.
- (S7) Yang, H.; Tang, Y.; Zou, S. Electrochemical removal of surfactants from Pt nanocubes. *Electrochem. Commun.* **2014**, *38*, 134-137.
- (S8) Hong, J. W.; Kim, Y.; Wi, D. H.; Lee, S.; Lee, S. U.; Lee, Y. W.; Choi, S. I.; Han, S. W. Ultrathin Free-Standing Ternary-Alloy Nanosheets. *Angew. Chem. Int. Ed.* **2016**, *55*, 2753-2758.
- (S9) Huang, W.; Kang, X.; Xu, C.; Zhou, J.; Deng, J.; Li, Y.; Cheng, S. 2D PdAg alloy nanodendrites for enhanced ethanol electrooxidation. *Adv. Mater.* **2018**, *30*, 1706962.
- (S10) Yang, Y.; Jin, L.; Liu, B.; Kerns, P.; He, J. Direct growth of ultrasmall bimetallic AuPd nanoparticles supported on nitrated carbon towards ethanol electrooxidation. *Electrochim. Acta* **2018**, *269*, 441-451.

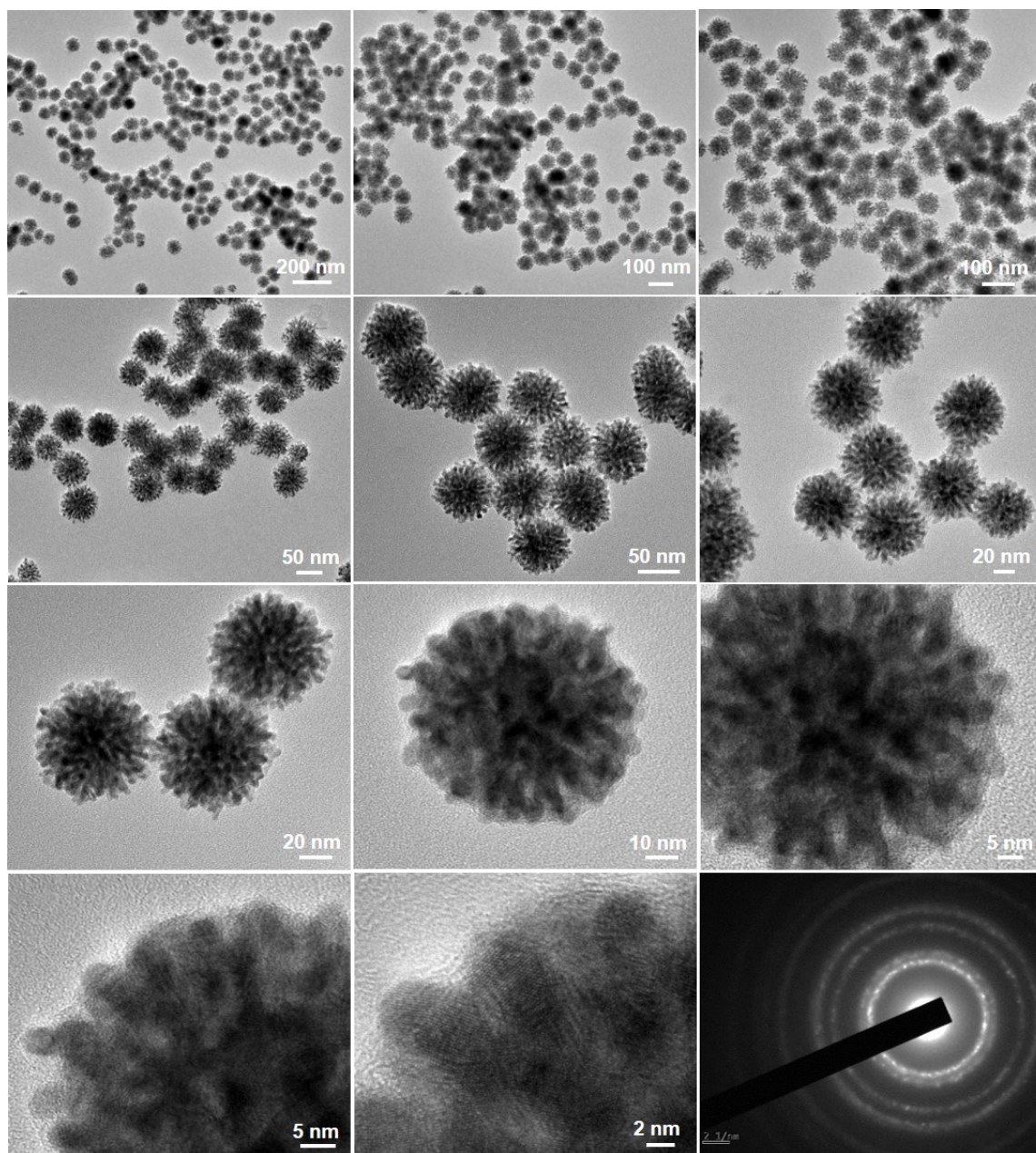


**Fig. S1** Supporting TEM images and SAED pattern of binary Pd-B MNSs with different magnifications.

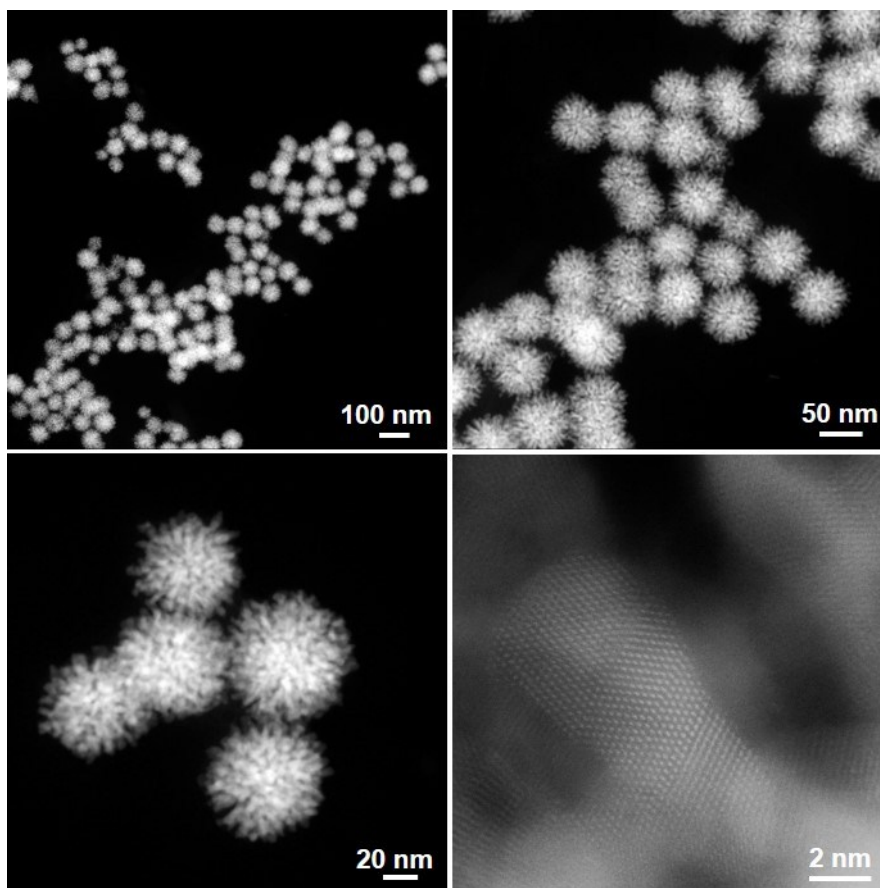


**Fig. S2** HAADF-STEM images of binary Pd-B MNSs with different magnifications.

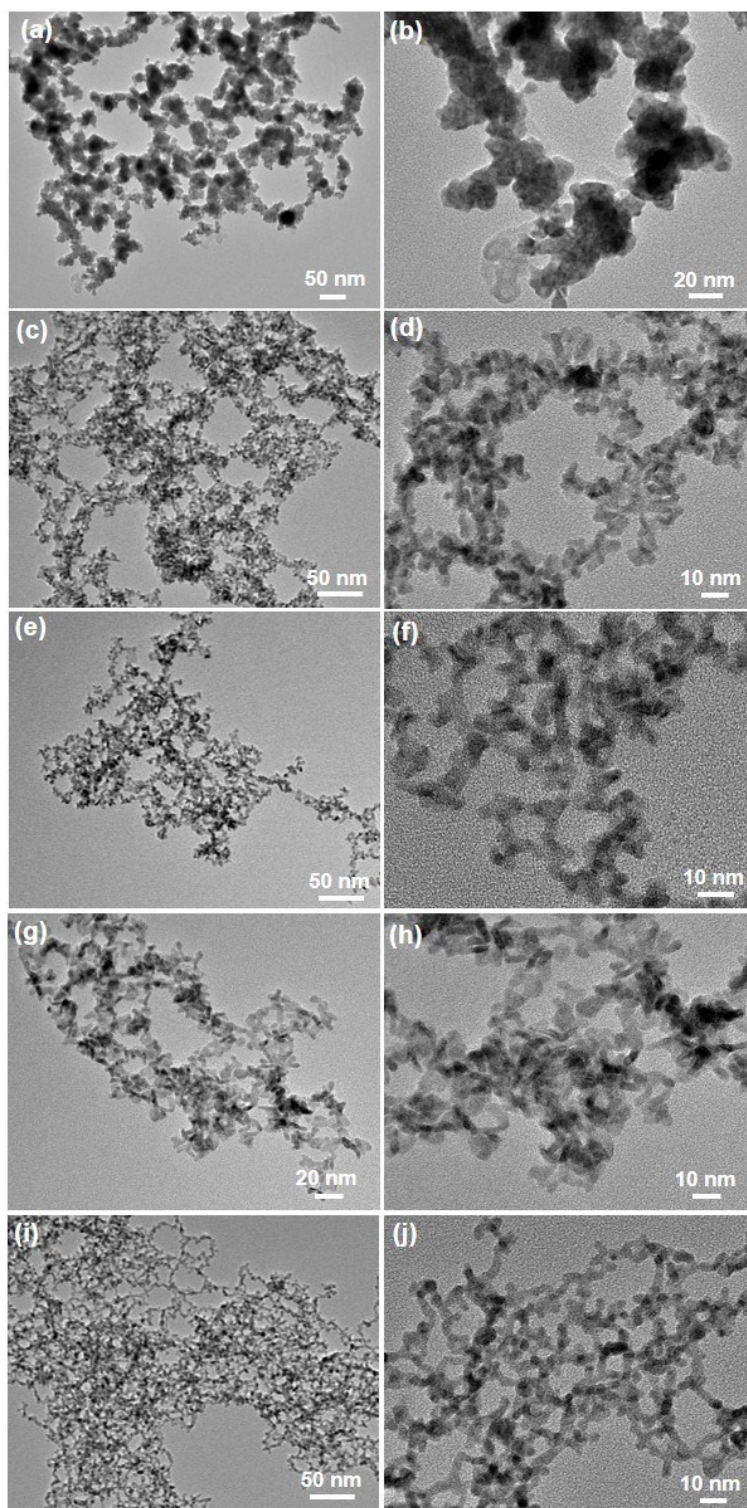


**Fig. S3** TEM images of binary Pd-B nanostructures synthesized (a, b) without the surfactant or with the surfactant of (c, d) C<sub>16</sub>TAC, (e, f) C<sub>18</sub>TAC, (g, h) C<sub>22</sub>TAC, and (i, j) Pluronic F127.

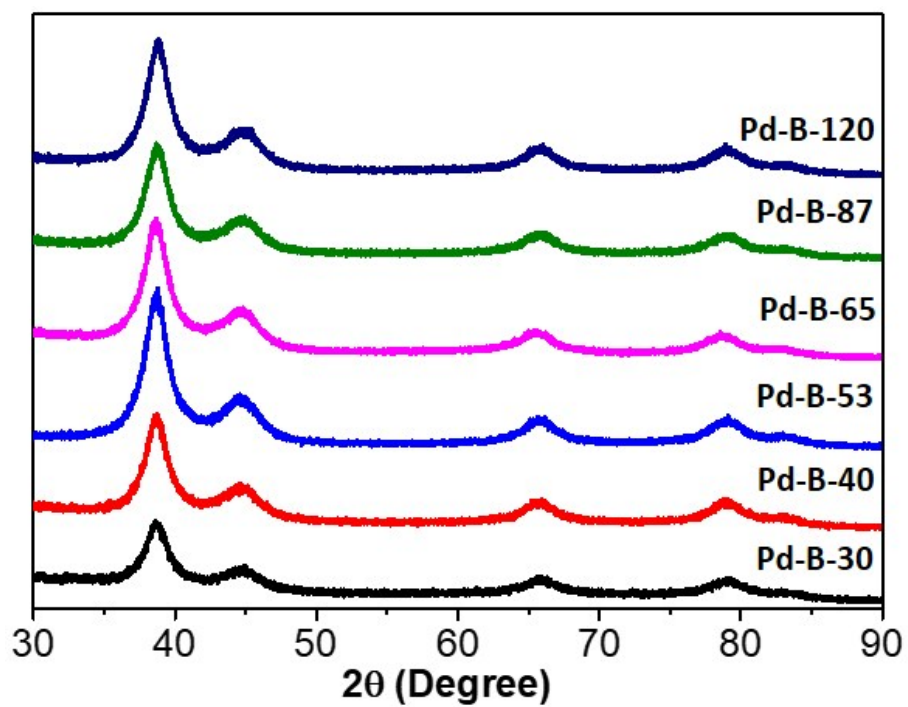


**Fig. S4** Wide-angle XRD patterns of binary Pd-B MNSs with different sizes synthesized under different pH of the reaction solution.

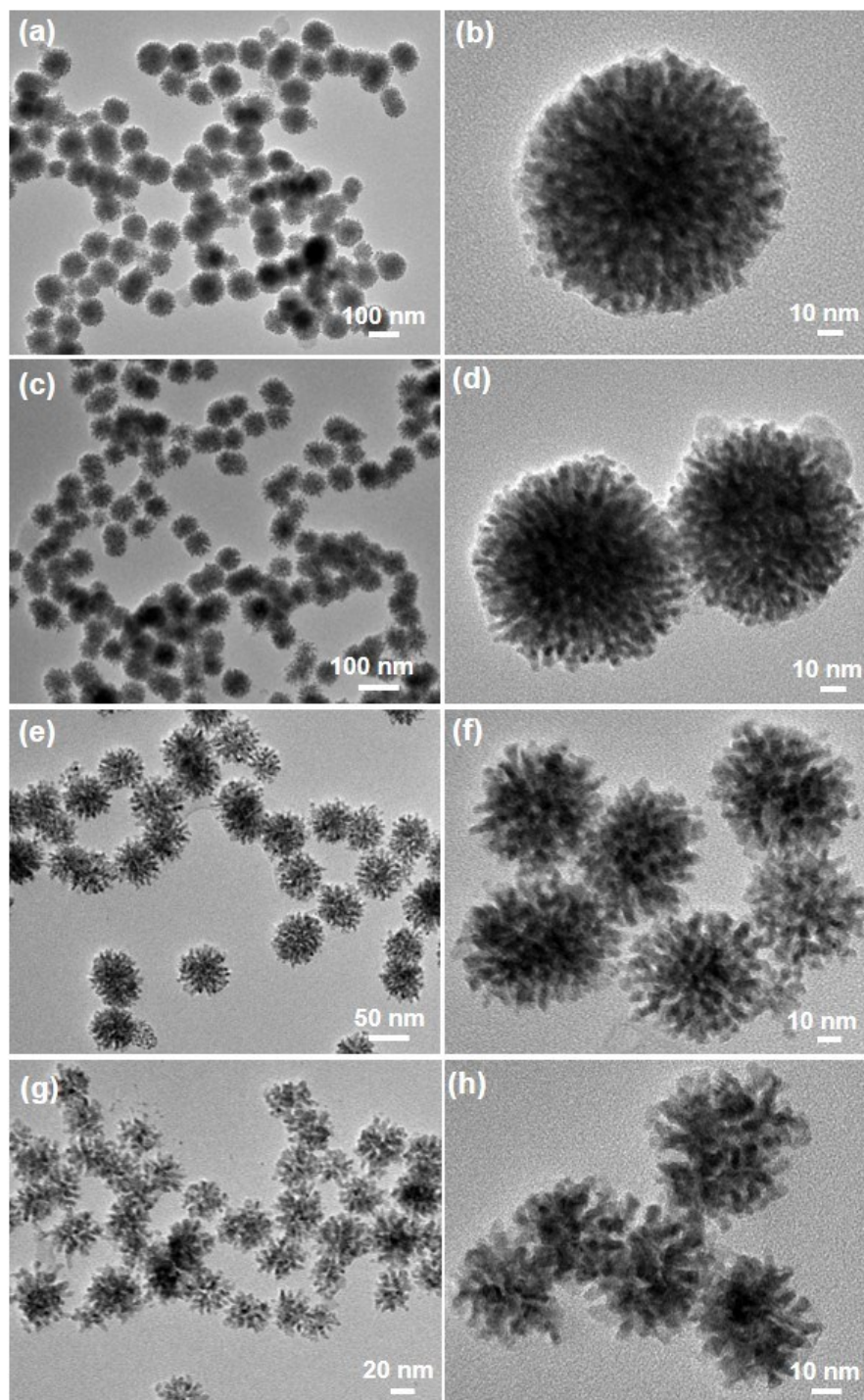


**Fig. S5** TEM images of binary Pd-B MNSs synthesized with different reaction temperature of (a, b) 50 °C, (c, d) 65 °C, (e, f) 85 °C, and (g, h) 95 °C. From the top to the bottom, the size of the Pd-B MNSs is 103 nm, 87 nm, 49 nm, and 32 nm, respectively.

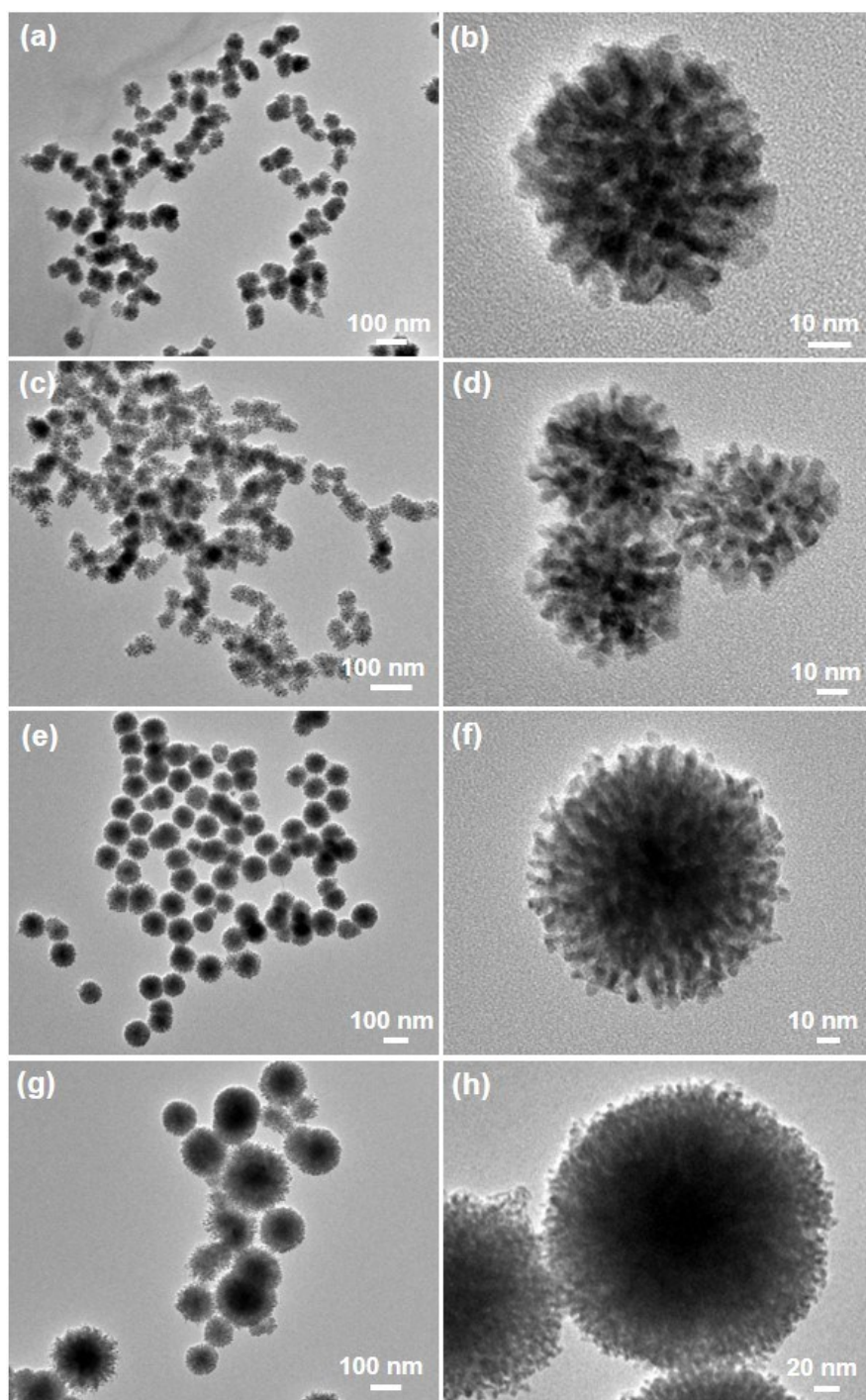


**Fig. S6** TEM images of binary Pd-B MNSs synthesized with different DODAC concentration of (a, b) 0.3 mg/mL, (c, d) 1.0 mg/mL, (e, f) 6.0 mg/mL, and (g, h) 12.0 mg/mL.

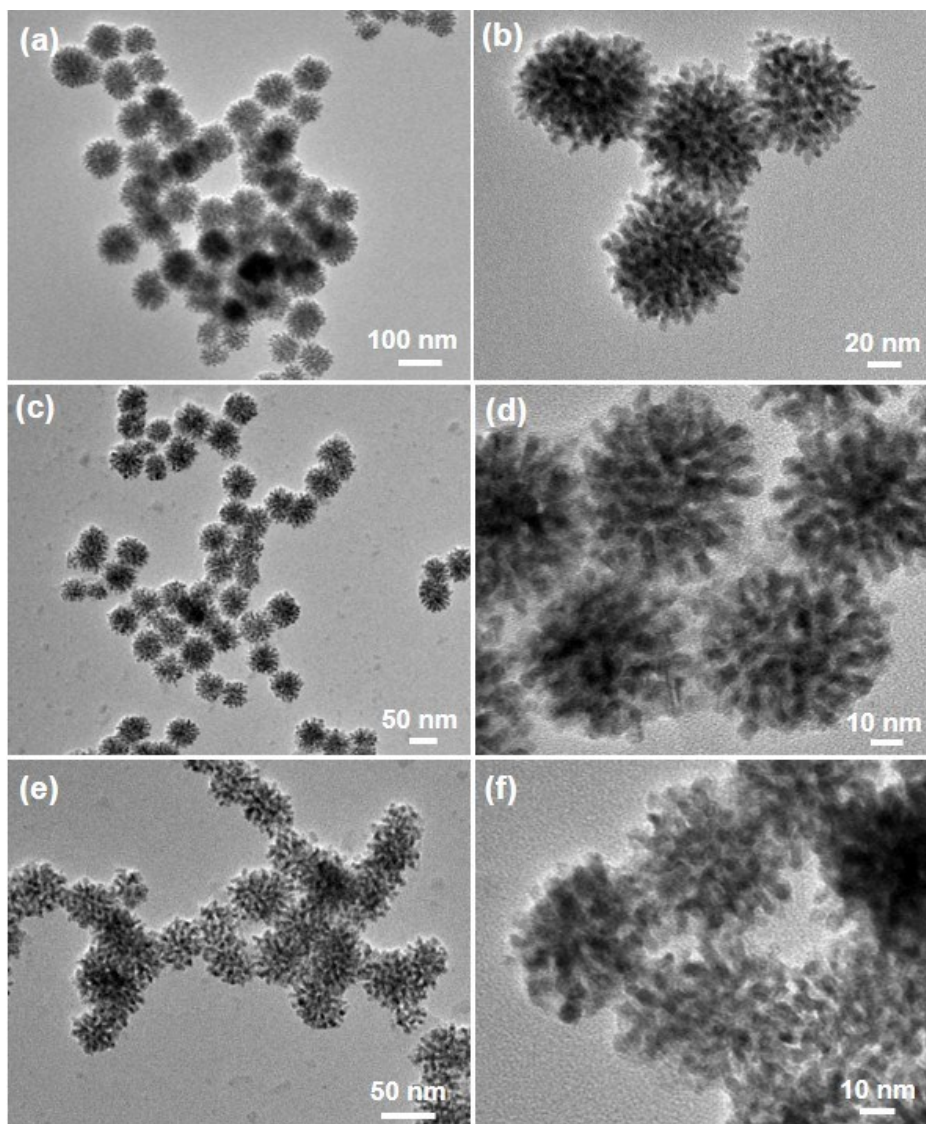


**Fig. S7** TEM images of binary Pd-B MNSs synthesized with different H<sub>2</sub>PdCl<sub>4</sub> concentration of (a, b) 0.4 mM, (c, d) 1.6 mM, and (e, f) 3.2 mM. From the top to the bottom, the size of Pd-B MNSs is 81 nm, 52 nm, and 39 nm, respectively.

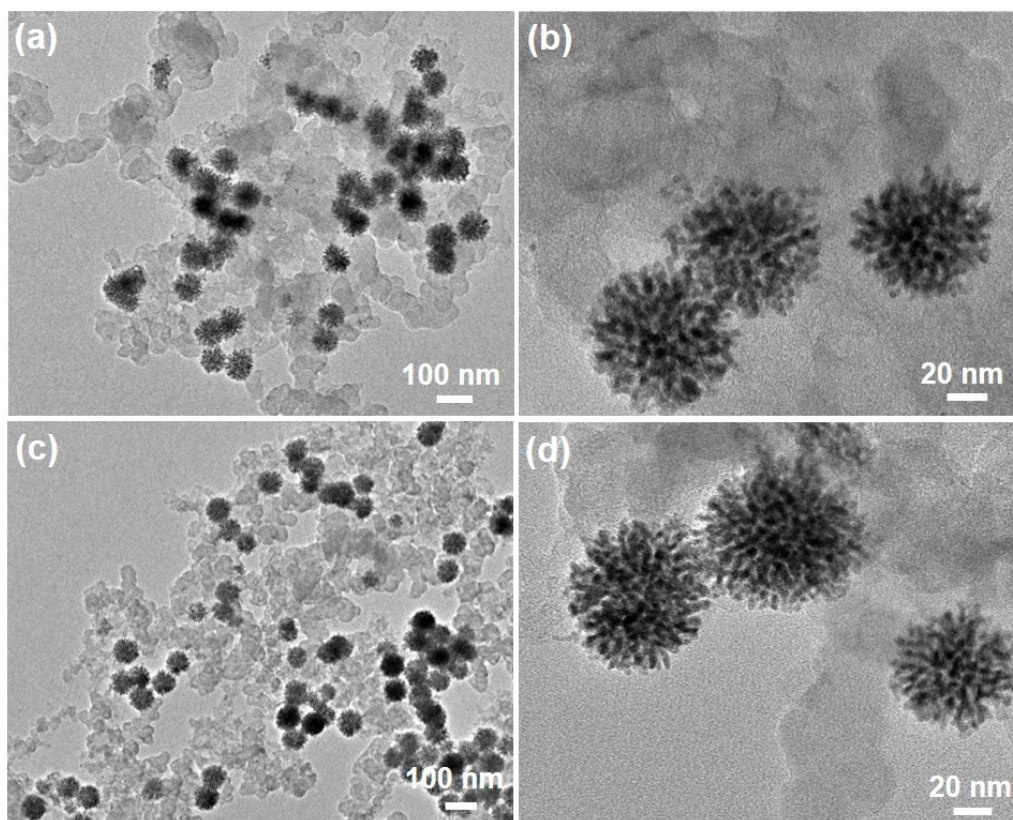


**Fig. S8** (a, b) TEM image of binary Pd-B MNSs loaded on Vulcan carbon, implying Pd-B MNSs well-dispersed on the supports without destroying the mesostructures. (c, d) TEM image of binary Pd-B MNSs after EOR stability test, indicating the superior structural stability. In order to evaluate the elemental composition of Pd-B MNSs after the electrocatalytic test, the molar ratio of Pd:B is checked by ICP and measured to be 84.1 : 15.9 (at. %), indicating good electrocatalytic and structural stability of Pd-B MNSs.

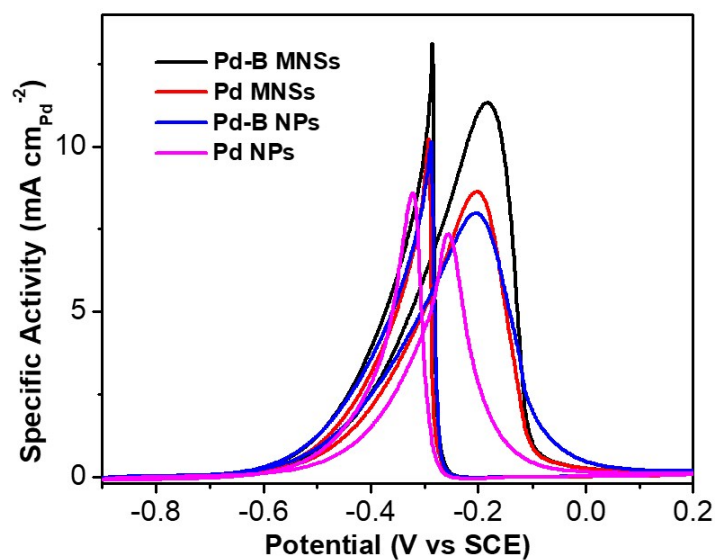


**Fig. S9** (a) CV curves binary Pd-B MNSs, Pd MNSs, Pd-B NPs and Pd NPs normalized to the ECSAs.

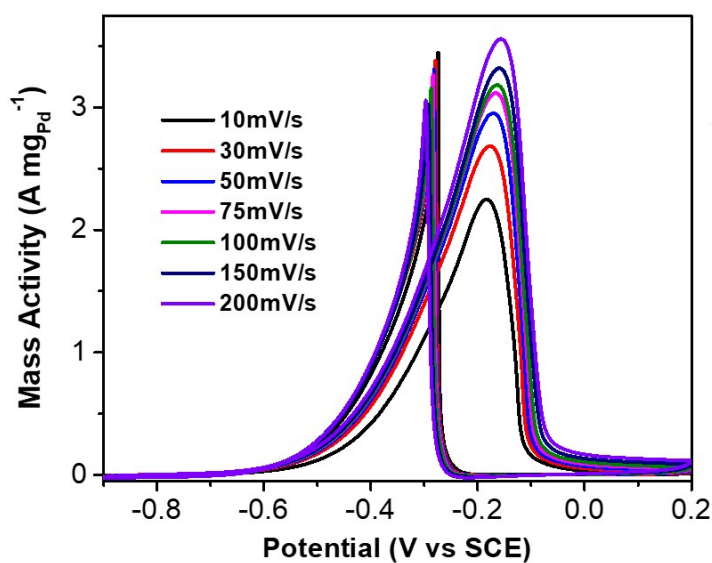


**Fig. S10** CV curves of the Pd-B MNSs with different scan rate ( $\nu$ ) of 10-200 mV s<sup>-1</sup> in 1.0 M KOH and 1.0 M ethanol.

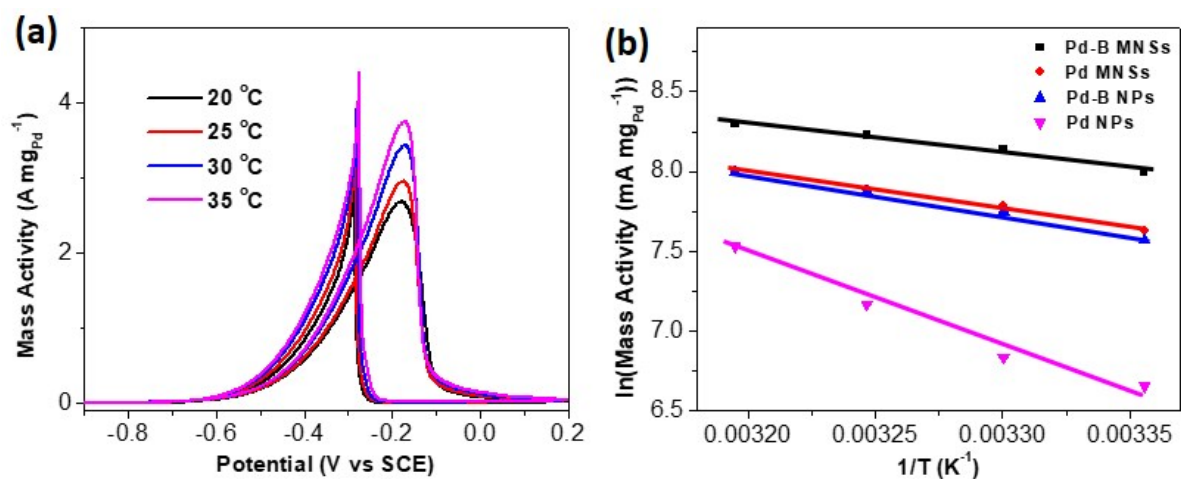


**Fig. S11** (a) CV curves of the Pd-B MNSs under different temperature of 20-40 °C in 1.0 M KOH and 1.0 M ethanol. (b) The relationship between mass activities and  $1/T$  (K<sup>-1</sup>) for Pd-B MNSs, Pd MNSs, Pd-B MPs and Pd NPs.

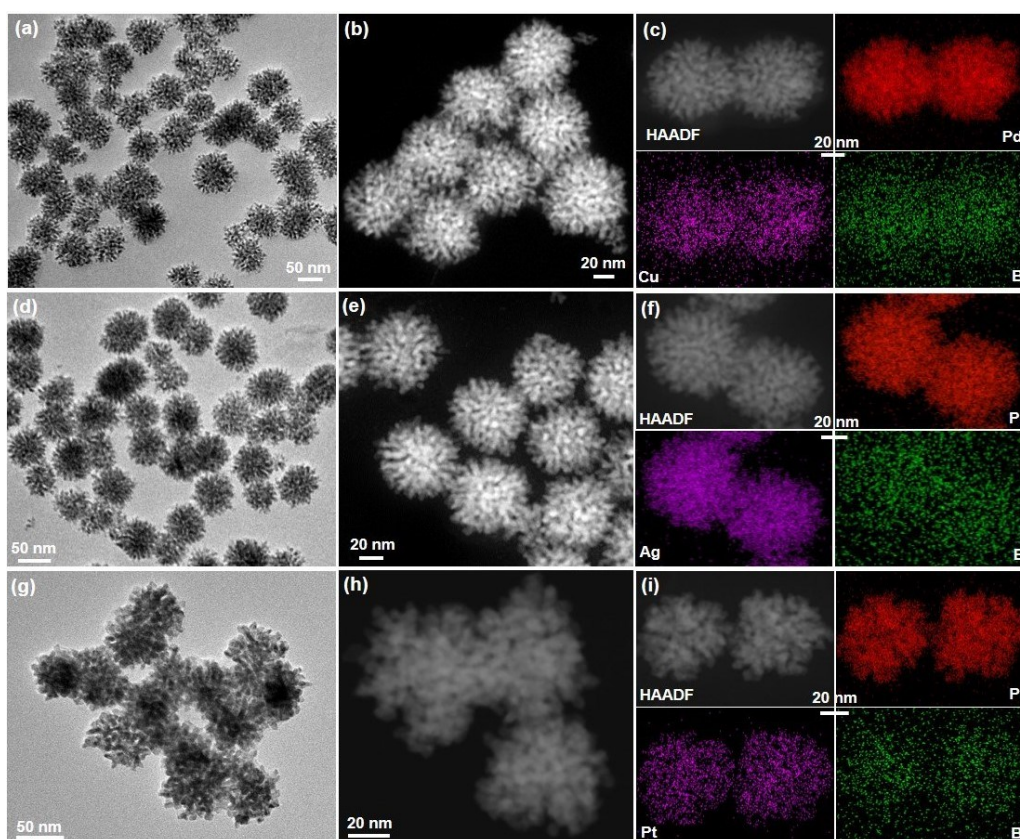


**Fig. S12** Typical TEM, HAADF-STEM images and STEM mappings of (a-c) ternary PdCu-B, (d-f) PdAg-B and (g-i) PdPt-B MNSs.

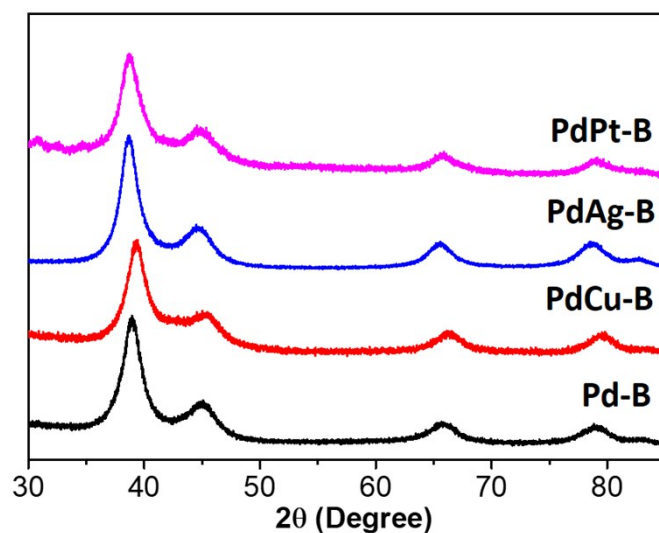


**Fig. S13** Wide-angle XRD patterns of ternary PdCuB, PdAgB and PdPtB MNSs.

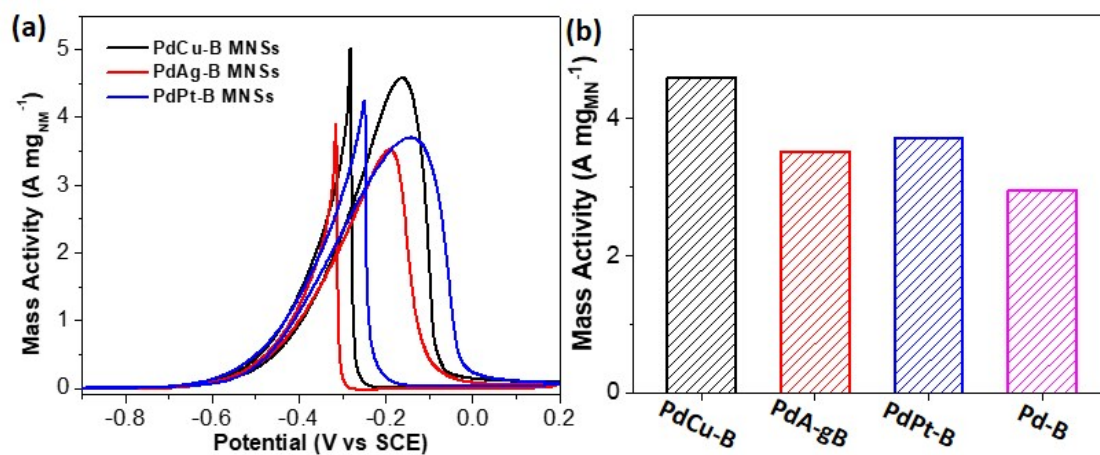


**Fig. S14** (a) CV curves and (b) summarized mass activities of ternary PdCuB, PdAgB and PdPtB (binary Pd-B MNSs as a control) in 1.0 M KOH and 1.0 M ethanol.

**Table S1.** Summarization of electrochemical EOR performance of Pd-based nanoalloys in alkaline solution.

Electrocatalyst	Electrolyte		Peak current from CV ( $A\ mg_{Pd}^{-1}$ )			Reference
	Ethanol	KOH	50 $mV\ s^{-1}$	100 $mV\ s^{-1}$	200 $mV\ s^{-1}$	
PdCu-B MNSs	1.0 M	1.0 M	4.62	4.97	5.38	This work
Pd-B MNSs	1.0 M	1.0 M	2.95	3.25	3.57	This work
Au@PdAuCu MNSs	1.0 M	1.0 M	3.99	-	-	Green Chem. 2019, C9GC00263D
PdB/C	1.0 M	0.5		112.5 $mA\ cm^{-2\ c}$		J. Energy Chem, 2018, 27, 389
PdAg nanodendrites	1.0 M	1.0 M	- <sup>a</sup>	-	2.63	Adv. Mater. 2018, 30, 1706962
Pd <sub>4</sub> Au <sub>1</sub> -P/CNT	1.0 M	1.0 M	2.30	-	-	J. Catal. 2017, 353, 256
Au@Pd Nanorods	1.0 M	1.0 M	2.92	-	-	Adv. Mater. 2017, 29, 1701331
PdNiP NPs	1.0 M	1.0 M	-	4.95	-	Nat. Commun. 2017, 8, 14136
PdCo/N-doped Cabon	1.0 M	1.0 M	1.25	-	-	J. Mater. Chem. A 2017, 5, 10876
Pd <sub>3</sub> Pb nanoflowers	0.5 M	1.0 M	~0.51	-	-	J. Power Sources 2016, 301, 160
PdAg hollow nanoflowers	1.0 M	1.0 M	1.62	-	-	Chem. Eur. J. 2016, 22, 16642
PdCu <sub>2</sub> Nanoparticles	1.0 M	1.0 M	1.60	-	-	ACS Appl. Mater. Interfaces 2016, 8, 34497
Pd/Ru nanodendrites	1.0 M	1.0 M	1.15	-	-	Nanoscale 2015, 7, 12445
Pd-NiCoO <sub>x</sub> /C	1.0 M	0.5 M	~0.45	-	-	J. Power Sources 2015, 273, 631
PdNi Hollow Nanospheres	1.0 M	1.0 M	3.63	-	-	Angew. Chem. Int. Ed. 2015, 54, 1310
PdAg alloy network	1.0 M	1.0 M		1.97 <sup>b</sup>		ACS Appl. Mater. Interfaces 2015, 7, 13842
Pd <sub>7</sub> /Ru <sub>1</sub> nanodendrites	1.0 M	1.0 M	~1.15	-	-	Nanoscale 2015, 7, 12445
PdCo nanotube /carbon cloth	1.0 M	1.0 M	~1.50	-	-	Angew. Chem. Int. Ed. 2015, 54, 3669
Au@AgPd Nanoparticles	1.0 M	1.0 M	1.16	-	-	J. Phys. Chem. C 2015, 119, 18434
PdCu nanocapsules	1.0 M	1.0 M	1.14	-	-	Nanoscale, 2014, 6, 2768
Pd <sub>1</sub> Ag <sub>1</sub> NPs/GO	1.0 M	1.0 M	1.60	-	-	J. Power Sources 2014, 263, 13.
PdAg/rRO	1.0 M	1.0 M	~ 0.97	-	-	Electrochim. Acta 2014, 143, 207
10.8-nm-thick PdPt NWs	0.5 M	1.0 M	0.94	-	-	Adv. Mater. 2012, 24, 2326

<sup>a</sup>not provided,  
<sup>b</sup>not mentioned  
<sup>c</sup>Specific Activity